Rheol Acta
DOI 10.1007/s00397-005-0060-4

ORIGINAL CONTRIBUTION

Mohammad T. Islam

Prediction of multiple overshoots in shear stress during fast flows of bidisperse polymer melts

Received: 15 September 2005
Accepted: 25 October 2005

M. T. Islam (✉)
Department of Chemical Engineering,
University of Michigan,
Ann Arbor, MI 48109, USA
e-mail: Mohammad.Islam@Cytec.com
Tel.: +1-203-3212257
Fax: +1-203-3212643

Present address:
Cytec Industries Inc.,
Stamford, CT 06904, USA

Abstract We present a differential constitutive model of stress relaxation in polydisperse linear polymer melts and solutions that contains contributions from reptation, contour-length fluctuations, and chain stretching. The predictions of the model during fast start-up and steady shear flows of polymer melts are in accord with experimental observations. Moreover, in accordance with reported experimental literature (Osaki et al. in J Polym Sci B Polym Phys 38:2043–2050, 2000a), the model predicts, for a range of shear rates, two overshoots in shear stress during start-up of steady shear flows of bidisperse polymer melts having components with widely separated molar masses. Two overshoots result only when the stretch or Rouse relaxation time of the higher molar mass component is longer than the terminal relaxation time of the lower molar mass component. The "first overshoot" is the first to appear with increasing shear rate and occurs as a result of the stretching of longer chains. Transient stretching of the short chains is responsible for the early time second overshoot. The model predictions in steady and transitional extensional flows are also remarkable for both monodisperse and bidisperse polymer solutions. The computationally efficient differential model can be used to predict rheology of commercial polydisperse polymer melts and solutions.

Keywords Bidisperse polymer · Constitutive model · Multiple overshoots · Polydisperse constitutive model · Tube model · Differential model

Introduction

The pioneering tube-model theory proposed by de Gennes (1979) and subsequently developed by Doi and Edwards (1986) was remarkably successful in predicting the linear and nonlinear rheology of monodisperse entangled polymer melts and concentrated solutions. In this theory, the constraints imposed by surrounding polymer chains are replaced by a hypothetical "tube" thereby converting the many-body problem to a single chain in a tube. The reptative relaxation of polymer chains were confirmed experimentally using fluorescence microscopy (Perkins et al. 1994), video microscopy (Kas et al. 1994), dynamic secondary-ion mass spectrometry (Russel et al. 1993), neutron mapping (Bent et al. 2003), and molecular dynamics simulation (Kremer and Grest 1990).

The main shortcomings of the tube or the "reptation" model were its failure to provide accurate predictions during steady shear and start-up of steady shear deformation histories. To obtain semiqualitative and quantitative agreement with experimental data by overcoming the limitations, additional mechanisms of relaxation were proposed: (1) fluctuation-driven stretchings and contractions of the chain along the tube ("contour-length fluctuations") (Marrucci and Grizzuti 1988) and (2) release of the constraints due to the motion of surrounding chains ("constraint release") (Marrucci 1996; Ianniruberto and Marrucci 1996).

By incorporating contour length fluctuations, Milner and McLeish (1998) have successfully predicted the linear rheology of monodisperse polymer melts including the 3.4 scaling of the zero-shear viscosity with molecular weight. Recently, Mead et al. (1998) proposed an integral constitutive model ("MLD" model) by taking into account all the three relaxation mechanisms—reptation, chain retraction, and convective constraint release (CCR). Islam and Archer (2001) also combined all the three relaxation mechanisms

using a force balance argument and proposed a simpler differential constitutive model ("IA" model). Both MLD and IA models resulted in greatly improved predictions of steady state and transient rheological behavior (Mead et al. 1998; Islam and Archer 2001; Sanchez-Reyes and Archer 2003).

On the contrary, theories for polydisperse polymer melts are much less advanced although of utmost importance since all commercial polymers are essentially polydisperse. The major challenge with polydisperse polymers is to take into account the dynamics of neighboring chains of different lengths (i.e., different molar masses) on any single-test chain. The problem becomes an interrelated many-body problem, leading to computationally demanding set of complex equations. Fairly recently, Pattamaprom and Larson (2001) proposed an integral constitutive model to describe nonlinear rheology of polydisperse polymer melts using a simplified version of the MLD model ("toy MLD"). The predictions of this model are in fairly good agreement with experimental data for bidisperse polymers of comparable molecular weights in case of steady shear flows (Pattamaprom and Larson 2001). However, integral constitutive models are computationally not attractive especially if predictions are required for commercial polydisperse polymers. On the contrary, differential constitutive equations are computationally less demanding and therefore more amenable for extensions to polydisperse systems.

The validity of any constitutive model can be decisively tested if the predictions are compared to the results obtained using extreme material parameters or for severe experimental conditions (e.g., reversing step shear flow). The former can be accomplished by comparing the predictions for bidisperse polymer melts, with components having widely different molar masses and thereby possessing widely separated relaxation times. For example, unusual and spectacular experimental observations such as multiple overshoots in shear stress are reported during fast start-up of steady shear flows of bidisperse polymer melts having components possessing widely separated relaxation times (Osaki et al. 2000a; Kinouchi et al. 1976).

Our primary objective in this article is to present a differential constitutive model for entangled polydisperse polymer melts that includes all three primary relaxation mechanisms: reptation, stretching, and constraint release. To validate the model, we intend to predict the unusual multiple-overshoot phenomena reported by Osaki and coworkers (Osaki et al. 2000a; Kinouchi et al. 1976) and unearth the molecular origin of the spectacular observations. The successful comparisons would certainly push the limits of the applicability of the tube model concept in general. In addition, the simple differential model would provide a platform for accurately predicting the rheological responses of commercial polydisperse polymer melts.

Model Development

Our starting point for formulating a differential model for polydisperse systems is the constitutive equations proposed by Islam and Archer (2001) ("IA" model, Eqs. (1), (3d), (4), and (5) of the reference). The premise of the present model is that the total stress is the weighted contribution of individual components of the polymer melt. The governing equation for time evaluation of polymer orientation is same as the original version (Eq. (1) of Islam and Archer 2001) except the fact that a separate expression has to be written for each individual component, "*k*".

$$\frac{\partial \mathrm{S}_{\mathrm{ij,k}}}{\partial \mathrm{t}}+\frac{1}{\tau_{\mathrm{d,k}}}\left(\mathrm{S}_{\mathrm{ij,k}}-\mathrm{S}_{\mathrm{ij,k,0}}\right)-\mathrm{S}_{\mathrm{ip,k}}\kappa_{\mathrm{jp,k}}-\kappa_{\mathrm{iq,k}}\mathrm{S}_{\mathrm{qj,k}} +\frac{1}{3}\left(\mathrm{S}_{\mathrm{ij,k}}\mathrm{S}_{\mathrm{pq,k}}+\mathrm{S}_{\mathrm{ip,k}}\mathrm{S}_{\mathrm{jq,k}}+\mathrm{S}_{\mathrm{iq,k}}\mathrm{S}_{\mathrm{jp,k}}\right)\mathrm{D}_{\mathrm{pq,k}}=0 \tag{1}$$

Here, $D_{\mathrm{pq}}=(1/2)\,(\kappa_{\mathrm{pq}}+\kappa_{\mathrm{qp}})$, κ is the deformation gradient tensor, and $S_{ij}=\langle u_i u_j\rangle$ is the second moment tensor of the segment orientation vectors, where the angular brackets signify averages over configuration space.

Acceleration of relaxation dynamics of polymer chains are taken into account by introducing the concept of modified reptation or modified terminal relaxation time:

$$\frac{1}{\tau_{d,k}}=\frac{1}{\widehat{L}_k^3\tau_{d0,k}}+\frac{1}{\widehat{L}_k^3}\left(\sum_m w_m\kappa_{ij,m}S_{ji,m}-\frac{1}{\widehat{L}_k}\frac{\partial\widehat{L}_k}{\partial t}\right). \tag{2}$$

For each component *k*, the second and third terms (terms inside the bracket) represent loss of entanglement constraints due to the convective motion of all chains (the sum "*m*" is over all different size fractions) relative to the change in length of the chain type, *k*. In Eq. (2), $\widehat{L}_k=\overline{L}_k/\overline{L}_{\mathrm{o},k}$, $\overline{L}_k$, and $\overline{L}_{o,k}$ are the average contour length of the primitive chain type *k* under flow and in the absence of flow, respectively.

In case of fast flows, evolution of the contour length of the primitive chains plays a dominant role. The length evolution or stretch rate of size fraction *k* can be expressed in terms of the following expression:

$$\frac{\partial\widehat{L}_k}{\partial t}=\frac{\Phi\left(\widehat{L}_k\right)}{\tau_{\mathrm{R,k}}}\left(1-\widehat{L}_k\right)+\widehat{L}_k\kappa_{ij,k}S_{ji,k}+\frac{1}{2}\left(1-\widehat{L}_k\right) \left[\left(\sum_m w_m\kappa_{ij,m}S_{ji,m}-\frac{1}{\widehat{L}_k}\frac{\partial\widehat{L}_k}{\partial t}\right)+\sum_{\mathrm{m}} w_m\frac{1}{\widehat{L}_m^3\tau_{d0,m}}\right]. \tag{3}$$

The stretch elongation is slowed by the terms inside the square bracket. The first two terms represent contributions from CCR, where the third term is due to reptative constraint release caused by the reptation of chains of different sizes.

The CCR on test chain k will be due to the retraction of chain k with respect to the mesh of constraints surrounding the chain. The mesh of constraints is composed of all chain types "m." This is conceptually different from the way CCR was modeled in the Toy MLD model (Pattamaprom and Larson, 2001). In the MLD model, constraint release of test chain "i" (Eq. 3 of the reference) will depend on the retraction of all chain types "j" with respect to the convection of mesh of constraints. The present formalism is more appropriate since Eq. (3) represents the evolution of length or stretch rate of chain k, and it takes into account the CCR due to the matrix and flow parameters on the test chain (of type k). The contribution from all chain types is taken into account later in Eq. (5).

In the present formulation, there is CCR if the test chain k is not stretching as fast as the tube in which it resides. Therefore, CCR may occur even if the surrounding chains are affinely deformed. In the MLD formulation, there is no CCR if the matrix chains deform affinely.

The $\Phi(\widehat{L}_k)$ function in the first term of Eq. (3) takes into account the finite extensibility of polymer chains (Pattamaprom and Larson (2001). The value of the function is unity for linear springs (at low deformation rates) but increases at higher deformation rates when the springs (polymer chains) become fully stretched. $\Phi(\widehat{L}_k)$ can be approximated by the normalized Padé Inverse Langevin function (Pattamaprom and Larson 2001; Cohen 1991).

$$\Phi(\mathrm{L}) = \frac{\left[3 - \left(\frac{\mathrm{L}}{\mathrm{L_{max}}}\right)^2\right] \Big/ \left[1 - \left(\frac{\mathrm{L}}{\mathrm{L_{max}}}\right)^2\right]}{\left[3 - \left(\frac{\mathrm{L_{eq}}}{\mathrm{L_{max}}}\right)^2\right] \Big/ \left[1 - \left(\frac{\mathrm{L_{eq}}}{\mathrm{L_{max}}}\right)^2\right]} \tag{4}$$

Finally, the total stress tensor can be written as weighed sums of individual components.

$$\begin{aligned} \sigma_{ij} &= \sum_k \sigma_{\mathrm{ij,k}} \\ &= G \sum_k w_k \Phi(\widehat{L}_k) \left\langle \overline{L}_k^2 \Big/ \overline{L}_{k0}^2 \right\rangle \left\langle u_{i,k} u_{j,k} \right\rangle \\ &\approx \frac{15}{4} G_N \sum_k w_k \Phi(\widehat{L}_k) \widehat{L}_k^2 S_{ij,k} \end{aligned} \tag{5}$$

Again, the subscript k denotes a component of the polydisperse system having molecular weight M_k, weight fraction w_k, and stretch ratio, $\widehat{L}_k = \overline{L}_k / \overline{L}_{\mathrm{o},k}$. The subscript "$ij$" represents "$ij$ th" component of the stress tensor (σ) and the second moment of the segment orientation tensor (S). $G \equiv 3ckTb^2/a^2 = (15/4)\, G_N$, where G_N is the plateau shear modulus of the material.

In the limit of monodisperse system, the five equations (Eqs. 1, 2, 3, 4 and 5) reduce to the original constitutive equations of Islam and Archer (2001) developed for monodisperse systems, with the exception of the finite extensibility coefficient, $\Phi(\widehat{\mathrm{L}}_\mathrm{k})$, introduced here. In the linear viscoelastic regime, $\widehat{L}_k = 1$, $\frac{1}{\widehat{L}_k} \frac{\partial \widehat{L}_k}{\partial t} = 0$ (chains are unstretched), and $\kappa_{ij} S_{ji} = 0$ (no convection).

Discussion

We have compared the model predictions with the experimental findings of Osaki et al. (2000a) during start-up of steady shear flow of entangled bidisperse polymer mixtures. Some of bidisperse systems of Osaki et al. (2000a) are composed of two fractions with widely different molecular weights where the stretch or Rouse relaxation time of (τ_{RH}) the higher (H) molar mass fraction is longer than the terminal or longest relaxation time (τ_{d0L}) of the lower (L) molar mass fraction. For these systems, spectacular double overshoots in shear stress were observed during the start-up of steady shear flows at high shear rates (e.g., Figs. 4 and 5 of Osaki et al. 2000a).

The model parameters are chosen so as to closely resemble sample f80/f850 of Osaki et al. (2000a), the results of which are reported in Fig. 5 of the reference. The individual longest relaxation times of lower molar mass (L) and higher molar mass (H) components at mixed concentration (C_{tot}=0.11 g cm^{-3}) are not given in the reference. Hence, the time scale of the model predictions is normalized with $\tau_{d0H}[Wi = \dot{\gamma}\tau_{dH0}]$, the longest or terminal relaxation time of the higher molar mass component. The ratio of the terminal relaxation times of two components ($\tau_{\mathrm{d0H}}/\tau_{\mathrm{d0L}}$) is taken to be as the 3.4th power of their molar mass ratio, $\tau_{\mathrm{d0H}}/\tau_{\mathrm{d0L}} \sim (M_{\mathrm{wH}}/M_{\mathrm{wL}})^{3.4} \sim (8.24\times 10^6/7.06\times 10^5)^{3.4} \sim 4{,}248$. Other parameters required for the model predictions are evaluated using standard relations (Doi and Edwards 1986). The ratios of the terminal relaxation time and the longest Rouse relaxation time for higher ($\tau_{\mathrm{d0H}}/\tau_{\mathrm{RH}}$) and lower ($\tau_{\mathrm{d0L}}/\tau_{\mathrm{RL}}$) fractions are estimated to be three times the entanglement density ($\tau_{\mathrm{d}}/\tau_{\mathrm{R}} \sim 3M/M_{\mathrm{e}}$) of that fraction (Doi and Edwards 1986). The molar mass between two neighboring entanglement points also known as the entanglement molar mass (M_{e}) is evaluated using the relation reported by Osaki et al. (2000a,b), (c, g cm^{-3})$^{1.4} M_{\mathrm{e}}(c)$=7,300 g mol^{-1}.

The values of the estimated parameters are as follows: mixed or total concentration, c=0.11 g cm^{-3}, M_{e} (c)=1.60×10^5 g mol^{-1}. $(M/M_{\mathrm{e}})_H \sim 51.3$, $(M/M_{\mathrm{e}})_L \sim 4.4$, $\tau_{\mathrm{d0H}}/\tau_{\mathrm{RH}} \sim 154$, and $\tau_{\mathrm{d0L}}/\tau_{\mathrm{RL}} \sim 13$. The weight fractions used for the model predictions are the same as used in

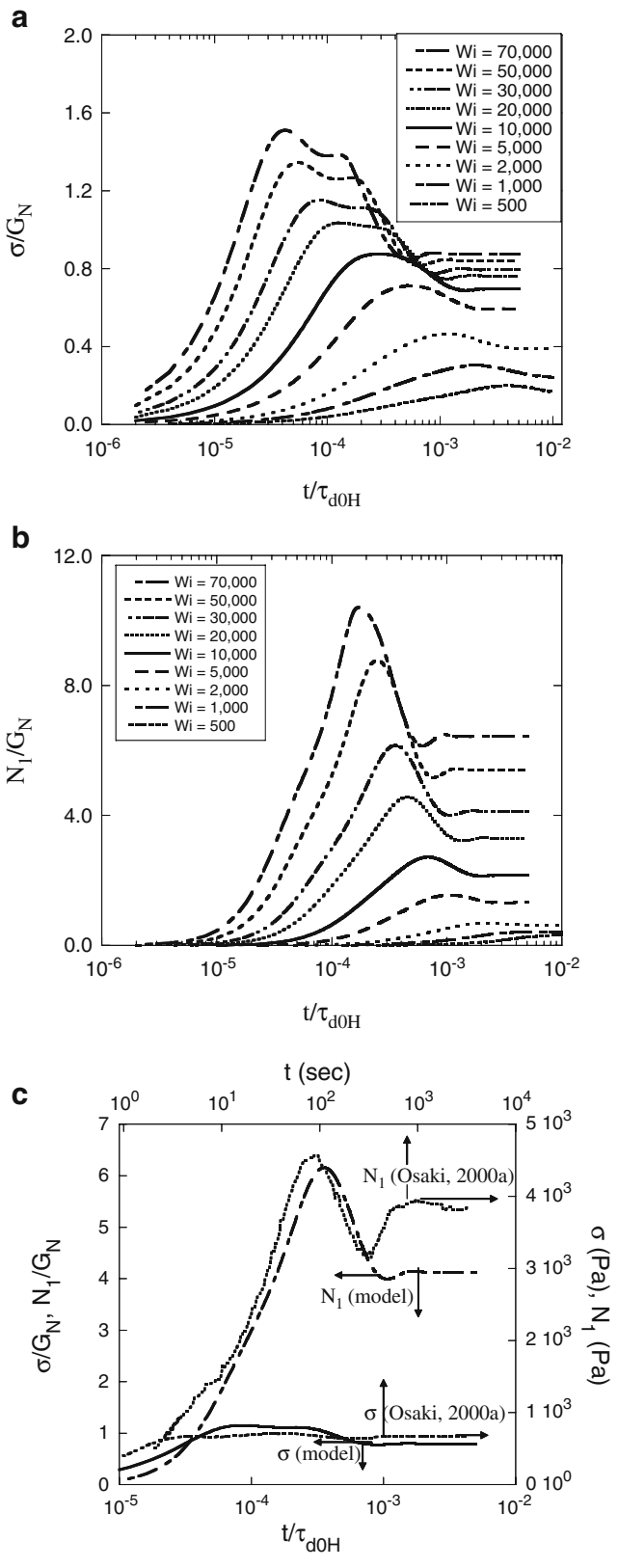

◀ **Fig. 1** Predictions for **a** shear stress (σ) and **b** first normal stress difference (N_1) for the bidisperse polymer melt during start-up of steady shear flow at different Wi[$=\dot{\gamma}\tau_{d0H}$]. **c** Comparison of the model predictions for W_i=30,000 with experimental data of Osaki et al. (2000a) for f80/f850 at $\dot{\gamma}$=0.58 s^{-1} (Fig. 5 of the reference) during start-up of steady shear flow

experiments, ω_H=0.01/(0.01+0.10)=0.091 and ω_L=1−ω_H=0.909.

The model predictions for shear stress (σ) and first normal stress difference (N_1) during start-up of steady shear flows are plotted in Fig. 1a,b. The abscissa and ordinate of the figures are normalized with τ_{d0H} and G_N (plateau modulus), respectively. The start-up profile including the appearance of a second overshoot in shear stress at high deformation rates is strikingly similar to Fig. 5 of Osaki et al. (2000a). This "second overshoot" is the second to appear with increasing shear rate. Similarities are also observed in case of other samples. Fig. 1c shows direct comparison between the model predictions for *Wi*=30,000 and the experimental data from Osaki et al. (2000a) obtained for $\dot{\gamma}$ =0.38 s^{-1}. The model is able to qualitatively predict the overshoot as well as the undershoot in N_1. It also

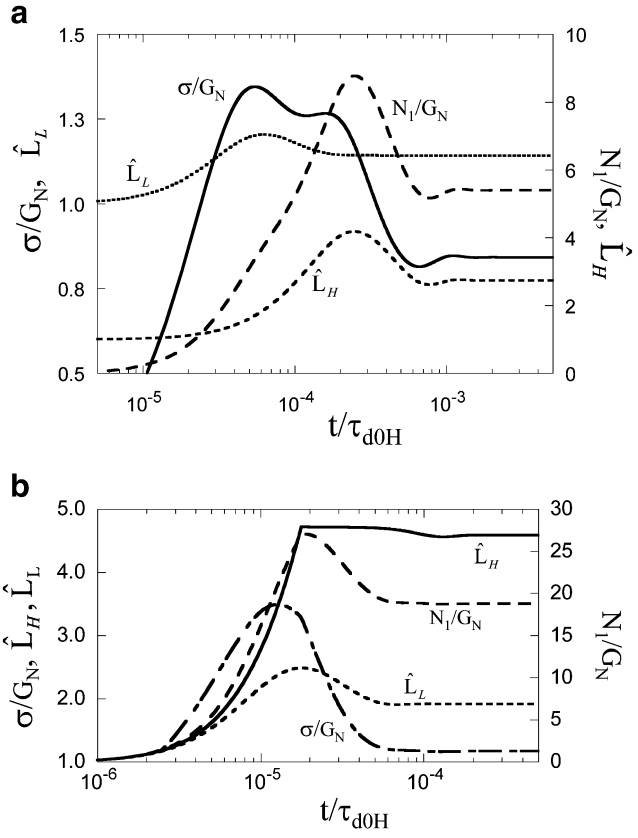

Fig. 2 Normalized shear stress (σ/G_N), first normal stress difference (N_1), and stretch ratio of higher ($\hat{L}_L$) and lower ($\hat{L}_H$) molar mass components during start-up of steady shear flow at **a** *Wi* [$=\dot{\gamma}\tau_{d0H}$]= 50,000 and **b** *Wi*=500,000

predicts the two overshoots in σ. However, the model over predicts the magnitudes of the overshoots in both σ and N_1.

The model predictions can be used to gain insight as to the origin of the two overshoots in shear stress for example at Wi=50,000. The transient dynamics of the normalized primitive length ($\widehat{L}$) for each fraction are plotted along with σ and N_1 in Fig. 2a. As expected, the longer time first overshoot in σ and the overshoot in N_1 are primarily due to the transient stretching of the higher molar mass fraction ($\widehat{L}_H$) chains. Comparison of the maxima in Fig. 2a suggests that the second overshoot at shorter time is due to the transient peak in $\widehat{L}_L$. According to this argument, the second overshoot in σ should start to appear approximately when $\dot{\gamma} \sim \tau_{RL}^{-1}$, i.e., $Wi \sim \tau_{d0H}/\tau_{RL} \sim (\tau_{d0H}/\tau_{d0L})(\tau_{d0L}/\tau_{RL}) \sim$ 4,248×13~55,000. This argument is also in agreement with the reasoning suggested by Osaki et al. (2000a) for the appearance of the second overshoot. It is important to note that the relative magnitudes or widths of the overshoots, i.e., whether the second overshoot appears as a peak, a kink, or a shoulder, depend on the values of several parameters: the mass (w_H/w_R) and molar mass (M_{wH}/M_{wL}) ratios of two fractions and the entanglement density (M_H/M_e, M_L/M_e) of each component.

It is also noteworthy to mention that the proposed model, with only two parameters (τ_{d0} and τ_R) for each component, is able to predict subtle features such as undershoots in σ and N_1 (Fig. 2a) that immediately follow the overshoots at high W_i.

Due to practical experimental limitations such as edge fracture, slip, and other artifacts, it is usually not possible to perform start-up measurements at even higher Wi than reported by Osaki et al. (2000a). Although use of standard polystyrene with higher molar mass (e.g., M_{wH}=20.6×10^6 g mol^{-1} instead of 8.24×10^6 g mol^{-1}) than used by Osaki et al. along with a suitable lower molar mass standard may make it possible to go even higher Wi or $\dot{\gamma}$, avoiding experimental limitations. Nevertheless, the model can be used to predict the dynamics at even higher Wi. As Wi (or $\dot{\gamma}$) is increased further (W_i>50,000), the transient overshoot in $\widehat{L}_L$ becomes more pronounced, and as a result, a second overshoot in N_1 starts to appear. Like the second overshoot in σ, the overshoot in N_1 can manifest itself as a peak, a

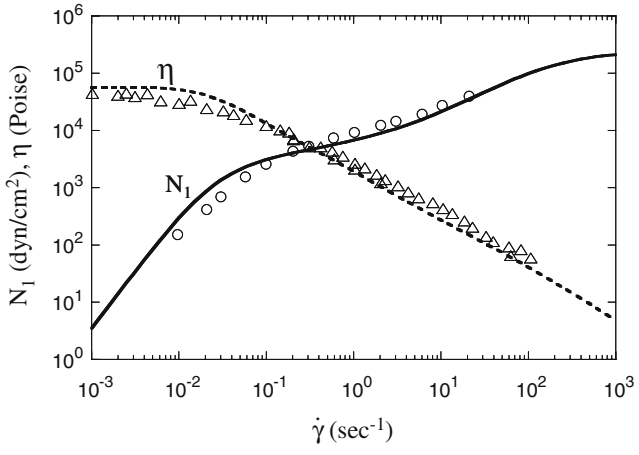

Fig. 3 Comparison of the steady-state shear viscosity η (*broken line*) and first normal stress difference N_1 (*solid line*) predicted by the model with experimental data for bidisperse polystyrene solution (molar masses 8.42×10^6 g mol^{-1} and 2.89×10^6 g mol^{-1} at a 60/40 ratio) reported in Fig. 10 of Pattamaprom and Larson (2001)

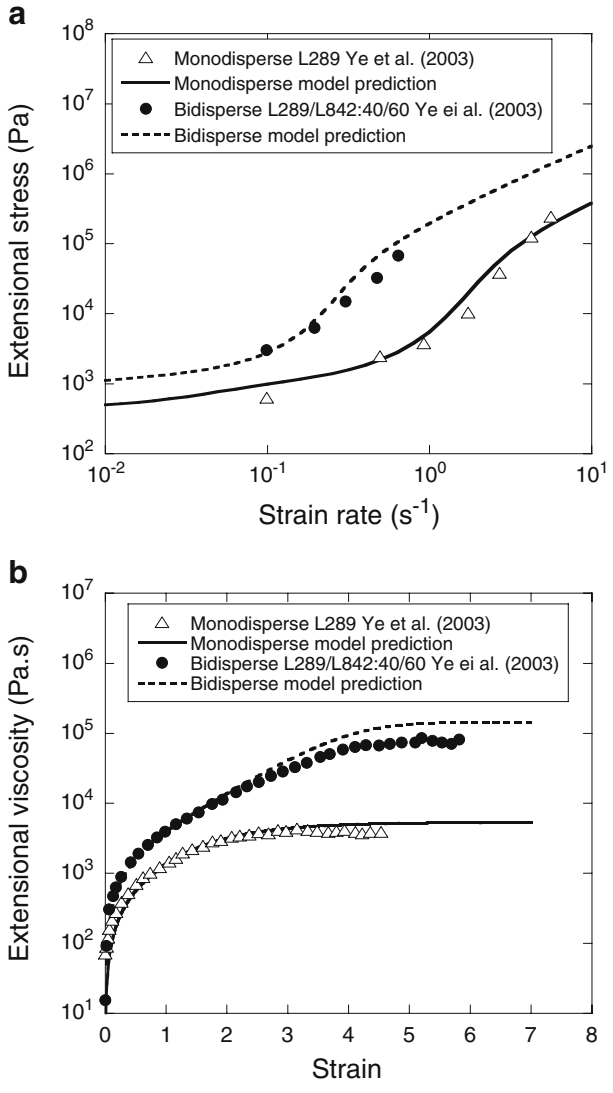

Fig. 4 **a** Comparison of the model predictions of the steady state extensional stress with the experimental monodisperse and bidisperse data from Ye et al. (2003) reported in Figs. 12 and 14c. The monodisperse system was polystyrene 2.89×10^6 g mol^{-1} (L289) dissolved in TCP at a volume fraction of 7%. The bidisperse mixture was composed of 40% L289 and 60% L842 (8.42×10^6 g mol^{-1}) dissolved in TCP at an overall polymer volume fraction of 7%. **b** Prediction of the transient extensional viscosity compared to the experimental monodisperse (L289-2.89×10^6 g mol^{-1} at 1 s^{-1}) and bidisperse (L289/L842-2.89×10^6/8.42×10^6 g mol^{-1}, 40/60 at 0.5 s^{-1}) polystyrene solution data from Ye et al. (2003) (Figs. 15 and 17c of the reference)

kink, or a shoulder depending on the mass ratio (ω_H/ω_R), molar mass ratio (M_{wH}/M_{wL}), or entanglement density of two fractions. For this particular bidisperse system, at even higher *Wi*, the higher molar mass polymer chain becomes fully stretched ($\widehat{L}_H \sim \widehat{L}_{H,\max}$) during start-up, and the first or longer time overshoot gradually disappears. The second overshoot remains as the only overshoot, which is due to the transient stretching of $\widehat{L}_L$. One such scenario is displayed in Fig. 2b where the time dependent values of the molecular parameters as well as stresses are plotted for *Wi*=500,000.

Next, we compare the predictions of the differential model with experimental data in case of steady shear flow of bidisperse polymer systems. For comparison, we have selected the recently published steady state data of Pattamaprom and Larson (2001) for entangled bidisperse polystyrene (PS) solutions in tricresyl phosphate (TCP). The mixture was composed of monodisperse fractions with molar masses 8.42×10^6 and 2.89×10^6 g mol^{-1} at 60/40 ratio. Same relaxation times (τ_d and τ_R for each component) evaluated in the reference (Pattamaprom and Larson 2001) were used to obtain the model predictions. A fairly good agreement is obtained between the model predictions and experimental data as displayed in Fig. 3. The magnitudes of σ_{ss} or η_{ss} ($\eta_{ss}=\sigma_{ss}/\dot{\gamma}$) and $N_{1,ss}$ predicted by the present model are found to be in-between the values predicted by toy MLD and "DEMG" models for polydisperse polymers (Pattamaprom and Larson 2001).

We conclude this paper by showing the remarkable predictions of the differential model in steady (Fig. 4a) and transitional (Fig. 4b) extensional flows for both monodisperse and bidisperse polymer solutions. The recently published extensional rheological measurements of monodisperse and bidisperse polystyrene solutions by Ye et al. (2003) are used for comparison. In Fig. 4a,b, comparisons are shown for data obtained from monodisperse polystyrene 2.89×10^6 g mol^{-1} (L289) dissolved in TCP at a volume fraction of 7% and a bidisperse mixture of 40% 2.89×10^6 g mol^{-1} and 60% 8.42×10^6 g mol^{-1} (L842) dissolved in TCP at an overall polymer volume fraction of 7%. The predictions are equally good for other bidisperse mixtures with different compositions. The parameters used for the model predictions are the TM parameter set evaluated in the reference—for L289 G_N=349.6 Pa, τ_d=9.4 s, τ_R=0.76 s; for L842 G_N=480.4 Pa, τ_d=189.6 s, τ_R=5.0 s; and $\beta=L_{eq}/L_{max}$=0.12.

Given the fact that the results of comparisons between predictions of constitutive models and experimental data are sensitive to the choice of parameters as well as the polymer chosen and its number of entanglements (Pattamaprom and Larson 2001), the match of the proposed model predictions with experimental data from different sources in case of both steady shear and start-up of steady shear flows can be considered remarkable. A comprehensive comparison of the predictions with alternative models as well as with experimental data for well-defined bi-, tri-, and polydisperse samples would be worthwhile, but beyond the scope of the present work.

Most commercial polymer processes of interest utilize polydisperse polymer melts in complex flow geometries. Therefore, the need for a simple, computationally efficient, yet fairly accurate differential constitutive model cannot be overstated. The present approach is a step forward in that direction.

References

Bent J, Hutchings LR, Richards RW, Gough T, Spares R, Coates PD, Grillo I, Harlen OG, Read DJ, Graham RS, Likhtman AE, Groves DJ, Nicholson TM, McLeish TCB (2003) Neutron mapping polymer flow: scattering, flow-visualisation and molecular theory. Science 301:1691–1695

Cohen A (1991) A Padé approximant to the inverse Langevin function. Rheol Acta 30:270–273

de Gennes PG (1979) Scaling concepts in polymer physics. Cornell University Press, Ithaca

Doi M, Edwards SF (1986) The theory of polymer dynamics. Clarendon, Oxford

Ianniruberto G, Marrucci G (1996) On compatibility of the Cox–Merz rule with the model of Doi and Edwards. J non-Newton Fluid Mech 65:241–246

Islam MT, Archer LA (2001) Non-linear rheology of highly entangled polymer solutions in start-up and steady shear flow. J Polym Sci B Polym Phys 39:2275–2289

Kas J, Strey H, Sackmann E (1994) Direct imaging of reptation for semiflexible actin filaments. Nature 368(6468):226–228

Kinouchi M, Takahashi M, Masuda T, Onogi S (1976) Nihon Reoroji Gakkaishi 4:25

Kremer K, Grest GS (1990) Dynamics of entangled linear polymer melts: a molecular dynamics simulation. J Chem Phys 92:5057–5086

Marrucci G (1996) Dynamics of entanglements: a nonlinear model consistent with the Cox–Merz rule. J non-Newton Fluid Mech 62:279–289

Marrucci G, Grizzuti N (1988) Fast flows of concentrated polymers: predictions of the tube model on chain stretching. Gazz Chim Ital 118:179–185

Mead DW, Larson RG, Doi M (1998) A molecular theory for fast flows of entangled polymers. Macromolecules 31:7895–7914

Milner ST, McLeish TCB (1998) Reptation and contour-length fluctuations in melts of linear polymers. Phys Rev Lett 81:725–728

Osaki K, Inoue T, Isomura T (2000a) Stress overshoot of polymer solutions at high rates of shear; polystyrene with bimodal molecular weight distribution. J Polym Sci B Polym Phys 38:2043–2050

Osaki K, Inoue T, Isomura T (2000b) Stress overshoot of polymer solutions at high rates of shear. J Polym Sci B Polym Phys 38:1917–1925

Pattamaprom C, Larson RG (2001) Constraint release effects in monodisperse and bidisperse polystyrenes in fast transient shearing flows. Macromolecules 34:5229–5237

Perkins TT, Smith DE, Chu S (1994) Relaxation of a single DNA molecule observed by optical microscopy. Science 264(5160):822–826

Russel TP, Deline VR, Dozier WD, Felcher GP, Agrawal G, Wool RP, Mays JW (1993) Direct observation of reptation at polymer interfaces. Nature 365 (6443):235–236

Sanchez-Reyes J, Archer LA (2003) Relaxation dynamics of entangled polymer liquids in steady shear flow. J Rheol 47:469–482

Ye X, Larson RG, Pattamaprom C, Sridhar T (2003) Extensional properties of monodisperse and bidisperse polystyrene solutions. J Rheol 47:443–468